Overview of MR Diffusion Tensor Imaging and Spatially Normalized FDG-PET for Diffuse Axonal Injury Patients with Cognitive Impairments

Ayumi Okumura, Jun Shinoda, and Jituhiro Yamada

Summary

We detected and compared brain dysfunction areas using both magnetic resonance (MR) diffusion tensor imaging (DTI) and spatially normalized ^{18}F-fluorodeoxyglucose positron emission tomography (^{18}F-FDG-PET; statistical FDG-PET) for the patients with memory and cognitive impairments due to traumatic brain injury. A total of 70 diffuse axonal injury patients with memory and cognitive impairments (DAI patients) and 69 age-matched normal subjects were studied with DTI and statistical FDG-PET. All subjects underwent examinations with a 1.5-T Signa MRI system. We used a single-shot spin-echo echoplanar sequence for diffusion-tensor analysis. Tractographic results were analyzed with diffusion tensor visualization (dTV) software. The group analysis for fractional anisotropy (FA) was performed with the SPM99 software package. FDG-PET was performed on all patients. After PET imaging, statistical analysis using the easy Z-score imaging system (eZIS) was undertaken with processing steps that included smoothing, normalization, and Z transformation with respect to a normal database. The Z-score map was superimposed on a three-dimensional MRI brain scan. Group analysis was performed using statistical parametric mapping analysis. A decline of FA was observed around the corpus callosum in the DAI patients compared with that of normal subjects, and reduced glucose metabolism was seen in the cingulate association. These results suggest that the reduced metabolism in the cingulate cortex indicated deprived neuronal activation caused by the impaired neuronal connectivity that was revealed with DTI. Furthermore, the metabolic abnormalities in the cingulate cortex may be responsible for memory and cognitive impairments. Age-related cerebral metabolic and blood flow decline was observed in the anterior cingulate association. The clinical combination of DTI and statistical PET has a role in

Department of Neurosurgery, Chubu Medical Center for Prolonged Traumatic Brain Dysfunction, Kizawa Memorial Hospital, 630 Shimokobi, Kobi-cho, Minokamo, Gifu 505-0034, Japan

neuroimage interpretation for patients with memory and cognition impairments because its three-dimensional visualization allows more objective and systematic investigation.

Key words Diffuse axonal injury, Diffusion tensor imaging, eZIS, Tractography, FDG-PET SPM

Introduction

Cognitive and vocational sequelae are frequent complications after traumatic brain injury without obvious neuroradiological lesions. They may present as memory disturbance, impaired multitask execution, and loss of self-awareness. These symptoms have been attributed to diffuse brain injury and the diffuse loss of white matter or neural networks in the brain. There is currently no accurate method to diagnose and assess the distribution and severity of diffuse axonal injury. As computed tomography (CT) and magnetic resonance imaging (MRI) findings underestimate the extent of diffuse axonal injury and correlate poorly with the final neuropsychological outcome, this dysfunction tends to be clinically underdiagnosed or overlooked. Indirect evidence for loss of functional connectivity after nonmissile traumatic brain injury (nmTBI) has been provided by functional neuroimaging, such as positron emission tomography (PET). Most functional neuroimaging studies conducted after nmTBI have demonstrated that cognitive and behavioral disorders are correlated with some degree of secondary hypometabolism or hypoperfusion in regions of the cortex. To date, however, there has been no direct, in vivo demonstration of structural disconnections in patients with nmTBI who do not have macroscopically detectable lesions.

Diffusion tensor MRI (DTI), which measures diffusion anisotropy in vivo, is a promising method for noninvasively identifying the degree of fiber damage in various disease processes affecting the white matter. In biological systems, the diffusional motion of water is impeded by tissue structures such as cell membranes, myelin sheaths, intracellular microtubules, and associated proteins; motion parallel to axons or myelin sheaths is inhibited to a lesser degree than perpendicular motion, a phenomenon known as diffusion anisotropy. To reduce interindividual variability and to evaluate the whole brain objectively, a statistical normalizing method, MRI voxel-based analysis, has been developed.

We investigated which regions in the whole brain are commonly injured in nmTBI patients with cognitive impairments but no macroscopic lesions using voxel-based analysis of fractional anisotropy (FA), referred to as diffusion anisotropy. The advent of DTI has allowed interregional fiber tracking, called MR tractography, which reconstructs the three-dimensional trajectories of white matter tracts. The second purpose of our study was to investigate the clinical applicability of DTI in combination with spatially normalized ^{18}F-fluorodeoxyglucose positron emission tomography (FDG-PET).

Materials and Methods

Patient Population

We studied 70 patients in the chronic stage after they had suffered severe nmTBI and had recovered from their coma. All had sustained a high-velocity, high-impact injury in a motor vehicle accident. Their clinical features and the results of neuropsychological examinations are presented in Table 1. The study population was selected from among 157 consecutive nmTBI patients who entered the rehabilitation program of Chubu Medical Center. Patients with severe language or attention deficits that prevented neuropsychological testing were excluded from the study. Also excluded were patients with physiological deficits or neuroradiologically detectable lesions >1.6 cm^3, such as contusions, hematomas, or infarcts. Neuropsychological testing was performed within 2 weeks of obtaining MRI scans.

For the overall estimation of their global intellectual, mnemonic performance and attention, we administered the Wechsler Adult Intelligence Scale–Revised (WAIS-R) test, the Mini-Mental State Examination (MMSE), the Wechsler Memory Scale–Revised (WSM-R) test, and the Paced Auditory Serial Addition test (PASAT). For each of these tests, an adjusted performance score below the lower limit of the 95% tolerance interval of the normal population was considered indicative of pathology in this study. The controls were 69 sex- and age-matched normal subjects. Neither the patients nor the control subjects had a history of neurological or psychiatric disorders. All participants gave prior written informed consent. The protocol was approved by the Research Committee of the Kizawa Memorial Hospital Foundation.

MRI Scanning Protocol

All subjects underwent examinations with a 1.5-T Signa MRI system (GE Medical Systems, Milwaukee, WI, USA). We used a single-shot spin-echo planar sequence (TR/TE 10 000/79 ms, slice thickness 3 mm, field of view 25 cm^2, number of experiments 4, pixel matrix 128 × 128 pixels) for diffusion tensor analysis. Diffusion gradients (b = 1000 s/mm^2) were always applied on two axes simultaneously around the 180 pulses. Diffusion properties were measured along six noncollinear directions. Diffusion-weighted MR images were transferred to a workstation supplied by the manufacturer (Advantage Workstation, GE Medical Systems); structural distortion induced by large diffusion gradients was corrected based on T2-weighed echo-planar images (b = 0 s/mm^2). The six elements of the diffusion tensor were estimated in each voxel assuming a monoexponential relation between signal intensity and the b-matrix. Using multivariate regression analysis, the eigenvectors and eigenvalues ($\lambda_1 > \lambda_2 > \lambda_3$) of the diffusion tensor were determined. The FA maps were generated on a voxel-by-voxel basis as follows.

$$FA = \sqrt{3/2} \times \sqrt{[(\lambda_1 - MD)^2 + (\lambda_2 - MD)^2 + (\lambda_3 - MD)^2]} / \sqrt{(\lambda_1^2 + \lambda_2^2 + \lambda_3^2)}$$

Spatial Normalization and Voxel-Based Analysis Using the FA Map

Spatial normalization is an essential preprocessing step in voxel-based analysis. As the contrast of the FA map is different from that of T1- or T2- weighted template images provided with the statistical parametric mapping (SPM99) software package (Wellcome, Department of Cognitive Neurology, London, UK), we created the FA template from a control group of 10 normal subjects. T2-weighed echo-planar images of the normal controls were segmented into gray and white matter and cerebrospinal fluid using SPM99 software running in MATLAB 5.3 (Mathworks, Natick, MA, USA). The segmented white matter images in native space were transferred to the white matter templates using the residual sum of squared differences as the matching criterion. The parameter of the transformation was also applied to the corresponding FA map. The normalized FA maps were smoothed with an 8-mm full-width at half-maximum (FWHM) isotropic Gaussian kernel, and a mean image (FA template) was created. All FA maps in native space were then transferred onto the stereotactic space by registering each of the images to the FA template image. Normalized data were smoothed with an FWHM isotropic Gaussian kernel. Statistically significant differences between the patients and controls were tested with the SPM99 software package without global normalization. To test our hypotheses with respect to regionally specific group effects, we compared the estimates using two linear contrasts (increased or decreased FA in patients versus controls). The threshold was set to uncorrected $p < 0.001$; significance levels were set at corrected $p < 0.05$.

MR Tractography

Magnetic resonance (MR) tractography was made with diffusion tensor visualization software. For tractography of the corpus callosum, seed-volumes were located from the genu to the splenium through the body on reconstructed midsagittal images. For tractography of the fornix, seed-volumes were located in the column of the fornix on reconstructed coronal images. The FA value for stop criteria was 0.18. Tractographic results were overlaid on T2-weighted images.

PET Examination

The PET scanner used in this study was an ADVANCE NXi Imaging System (General Electric Yokokawa Medical Systems, Tokyo, Japan), which provides 35

transaxial images at 4.25-mm intervals. The in-plane spatial resolution (FWHM) was 4.8 mm. The scan mode was the standard two-dimensional mode. Subjects were placed in the PET scanner so the slices were parallel to the canthomeatal line. Immobility was checked by alignment of three laser beams, with lines drawn on the patient's face. Subjects fasted for at least 4 h prior to injection of FDG. An FDG dose of 0.12 mCi/kg was injected intravenously through the cubital vein over a period of 1 min. The subjects were comfortably seated with their eyes open and environmental noises kept to a minimum for approximately 40 min. After a 40-min rest, a $^{68}Ge/^{68}Ga$ rotating pin source was used to obtain 3-min transmission scans. Static PET scan was performed continuously for 7 min. A static scan reconstruction was performed with corrections for photon attenuation using data from the transmission scans, dead time, random, and scatter.

Images were processed and analyzed on a Microsoft workstation using MATLAB software (Mathworks, Sherborn, MA, USA), an easy Z-score imaging system (eZIS), and SPM99 software (courtesy of the Functional Imaging Laboratory, Wellcome Department of Cognitive Neurology, University College, London, UK).

Results

Table 1 shows the demographics of the traumatic brain injury patients and normal subjects. Patients in this study show almost 80% performance of memory and cognition compared with normal subjects.

Table 1. Demographic of traumatic brain injury patients and normal subjects

Factor	Patients	Normal
Mean age (years)	27.43 ± 12.09	28.23 ± 11.90
Sex		
Male	19	19
Female	4	4
Duration of impaired consciousness (days), mean ± SD	7.2 ± 8.6	—
Injury to MRI interval (months), mean ± SD	14.16 ± 16.2	—
WAIS-R		
Full scale IQ	80.4 ± 11.2	104.2 ± 14.1
Verbal IQ	84.6 ± 12.2	103.6 ± 12.9
Performance IQ	78.0 ± 13.5	105.2 ± 15.9
MMSE	26.3 ± 4.5	29.7 ± 0.8
WMS-R		
General memory	71.7 ± 14.6	106.3 ± 12.1
Delayed memory	66.5 ± 13.2	103.7 ± 9.8
Visual memory	71.0 ± 14.0	102.1 ± 7.5
Attention	85.3 ± 16.3	107.3 ± 7.2
PASAT	34.5 ± 10.6	46 ± 6.2

MRI, magnetic resonance imaging; IQ, intelligence quotient; WAIS–R, Wechsler Adult Intelligence Scale–Revised; MMSE, Mini-Mental State Examination; WMS–R, Wechsler Memory Scale–Revised; PASAT, Paced Auditory Serial Addition Test

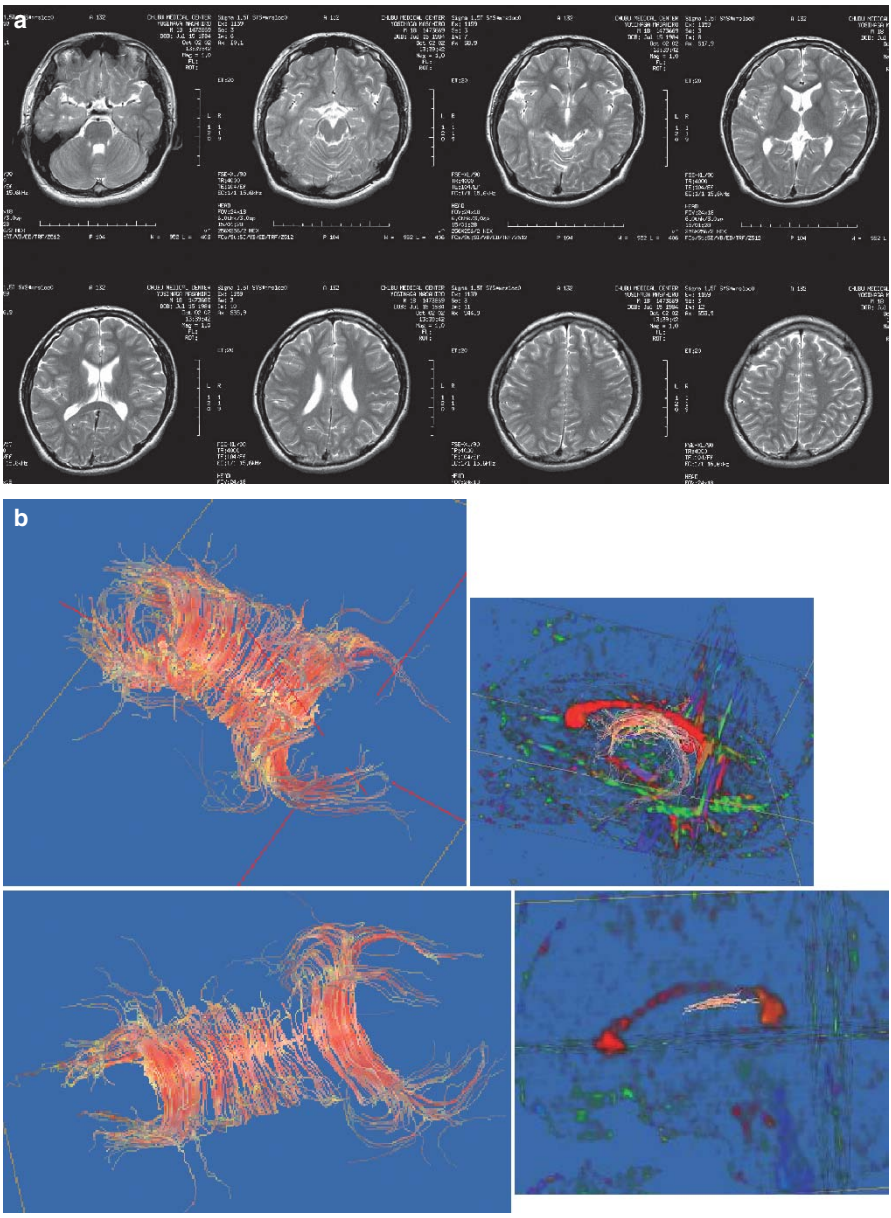

Fig. 1. **a** Conventional T2-weighted image (WI) of magnetic resonance imaging (MRI) of a traumatic brain injury patient (case 1) with cognitive impairment. There is no apparent abnormal lesion in this image. **b** Tractography of the corpus callosum and fornix of this patient compared to those of normal subjects

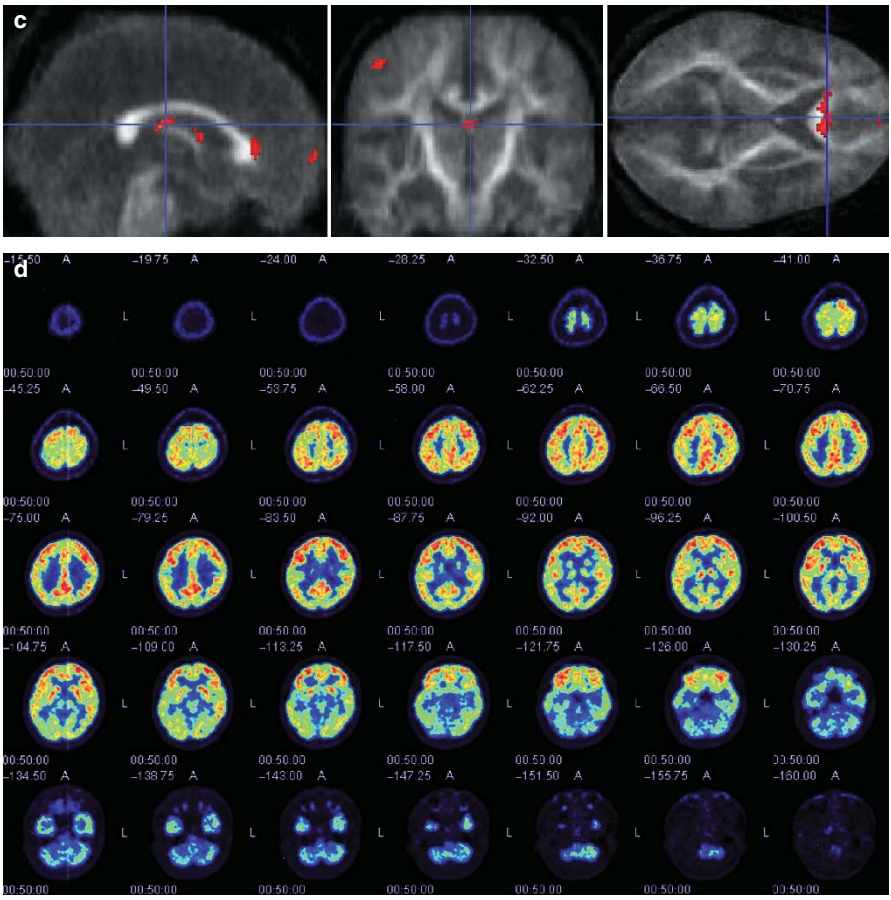

Fig. 1. **c** Fractional anisotropy (FA) reduction area on FA statistical parametric mapping (SPM) analysis. Red pixels show reduction of FA compared with normal. **d** Conventional fluorodeoxyglucose positron emission tomography (FDG-PET) of case 1. These images cannot display any metabolic abnormality

Figures 1 and 2 compare MR tractography of the corpus callosum and fornix of cases 1 and 2 (chosen from among the nmTBI cases) with that of normal subjects. In the nmTBI cases. the tracking lines through the genu and the body of the corpus callosum were thin and different from those of normal subjects, and the connecting fibers did not reach the frontal lobe. The volume and the connecting fibers from the splenium in the nmTBI patients were relatively retained. Compared to normal subjects, the nmTBI scans showed that the tracking lines through the column of the fornix were thin and did not pass along the fimbria of the hippocampus, although tractography around the mamillary body to the column of the fornix was relatively retained. An area of FA reduction was also seen around the corpus callosum and fornix (Fig. 1c).

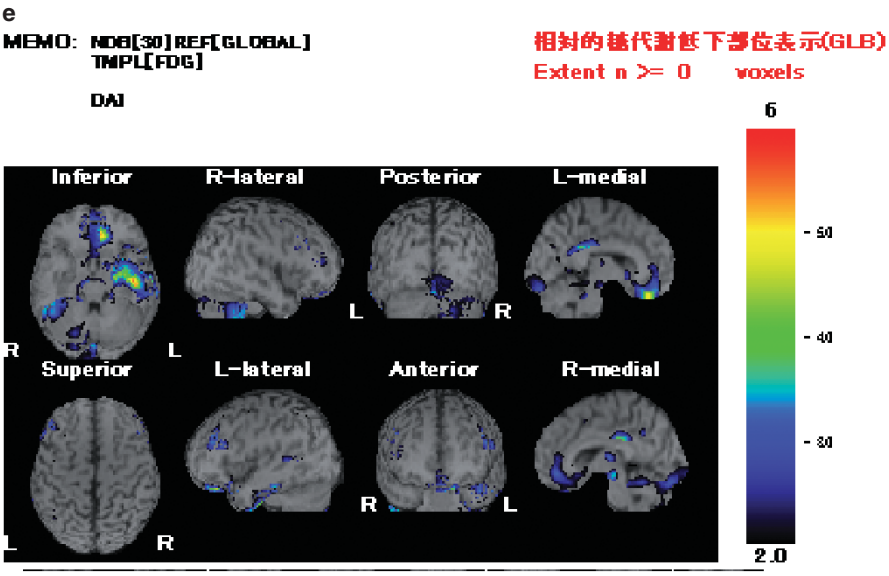

Fig. 1. **e** Easy Z-score imaging system (eZIS) reveals cerebral metabolic reduction in case 1. The areas of statistically significant reduction of metabolism are superimposed on brain surface images of each hemisphere. The color scale indicates the degree of significance (red > green > blue). This map shows abnormal metabolic voxels in posterior cingulate cortex

The eZIS views show cerebral metabolic reduction in these cases. Areas of statistically significantly reduced metabolism are superimposed on brain surface images of each hemisphere. The color scale indicates the degree of significance (red > green > blue). This map shows abnormal metabolic voxels in the posterior cingulate cortex.

In the group analysis, statistical parametric mapping (SPM) analysis indicated that the common area of FA reduction was the middle of the corpus callosum (Fig. 3). SPM analysis revealed the presence of significant hypometabolism in the medial prefrontal region, the medial frontobasal region, the anterior and posterior regions of the cingulate gyrus, and the thalamus bilaterally in all patients (Fig. 4) when compared with that of normal control subjects.

Discussion

Our results suggest that DTI was able to demonstrate objectively the abnormalities in nmTBI patients with cognitive impairments but no macroscopically detectable lesions. Voxel-based FA analysis objectively demonstrated the vulnerability of the corpus callosum and the fornix in nmTBI patients. The parasagittal subcortical white matter, internal capsules, cerebellar folia dorsal to the dentate nuclei, and the

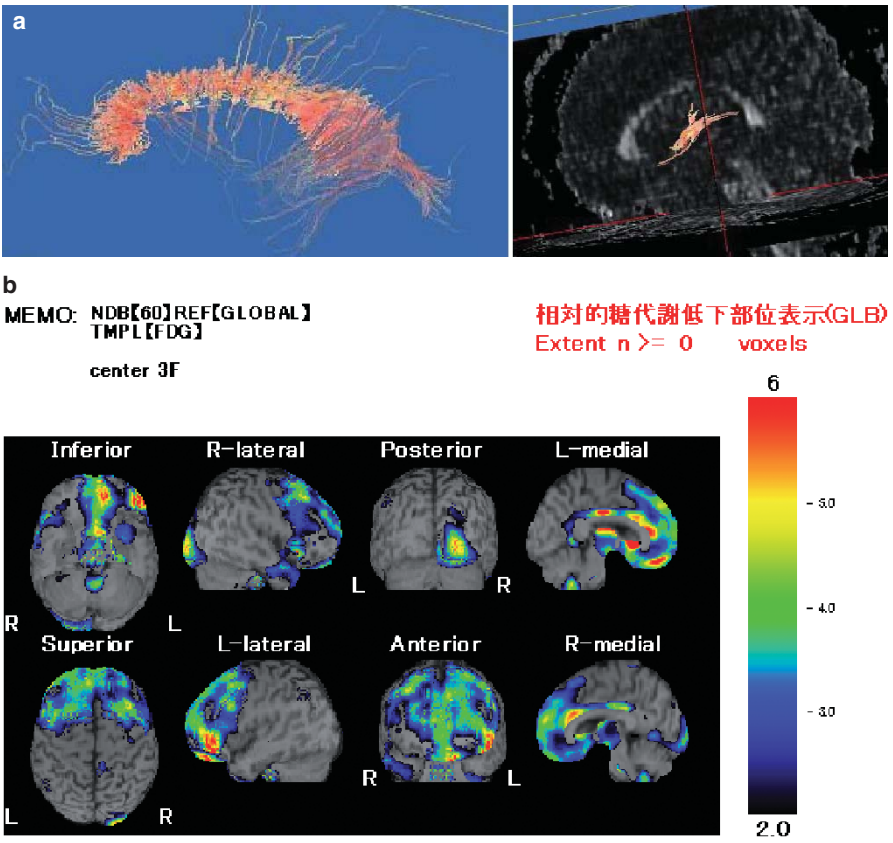

Fig. 2. **a** Tractography from the corpus callosum of case 2 patient, a 51-year-old man who was injured 8 months ago. Fibers from the corpus callosum of this case are coarse compared to those of a normal subject. **b** eZIS views of cerebral metabolic reduction in case 2. Areas of statistically significant reduced metabolism are superimposed on brain surface images of each hemisphere. The color scale indicates the degree of significance (red > green > blue). This map shows abnormal metabolic voxels in the anterior cingulate cortex

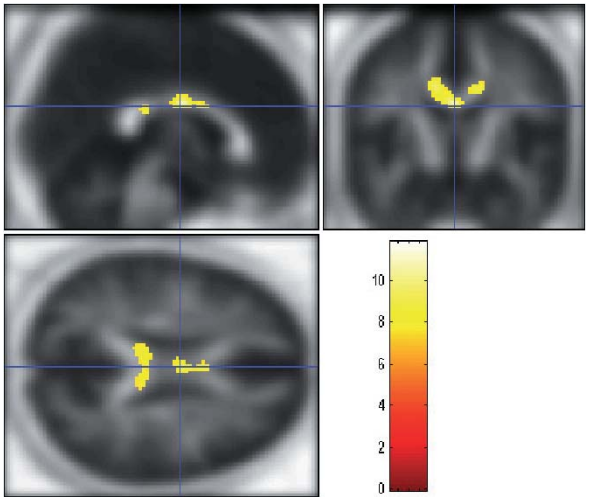

Fig. 3. SPM-rendered brain images of FA in normal subjects versus those of the diffuse axonal injury group

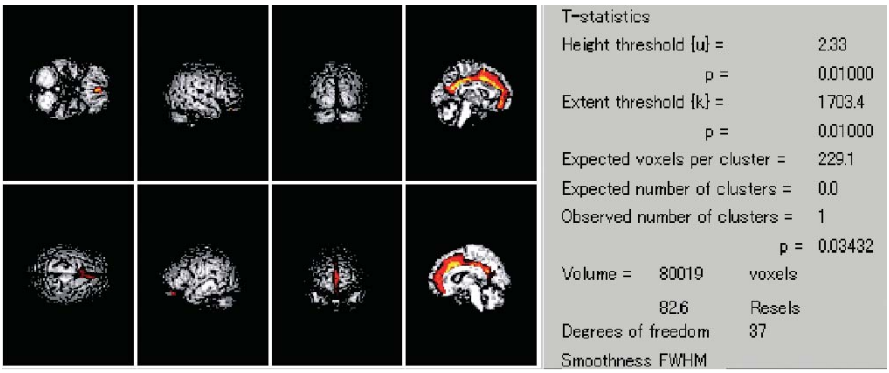

Fig. 4. SPM-rendered brain images of FDG-PET in normal subjects versus the diffuse axonal injury group. The orange areas represent statistical significance for a reduction in FDG in diffuse axonal injury group compared with controls. The spatial extent of orange cluster in voxels is located around the mesiofrontal cortex including the anterior cingulate association

brain stem, but not the corpus callosum or the fornix, are known to be susceptible to diffuse axonal injury. Our study was able to disclose the specific vulnerability of the corpus callosum and the fornix because our nmTBI patients had only cognitive impairments (no physiological problems).

The corpus callosum and the fornix are thought to be the structures at the core of the neural networks in cognition and memory. Changes in the anterior white matter, including the genu of the corpus callosum, are strongly related to age-related cognitive decline. The fornix is the major limbic white matter pathway interconnecting the hippocampus and the mamillary bodies. The limbic circuitry of the hippocampus–fornix–mamillary body interaction has been the focus of extensive research in memory function. Damage to any of these limbic structures results in various memory disorders.

The cingulate gyrus is a principal component of the limbic system, and its anterior and posterior parts have different thalamic and cortical connections and different cytoarchitecture, and they serve distinctive functions. The anterior cingulate gyrus can be divided into discrete anatomical and behavioral subdivisions: the affective division and the cognitive division. The affective division includes the areas of Brodmann 25 and 33 and the rostal area of Brodmann 24, and it plays a role in emotion and motivation; the cognitive division includes caudal areas of Brodmann 24 and 32 and plays a role in complex cognitive/attentional processing. Previous research indicates that significant regions of age-related decline remain prominent in the prefrontal cortex as well as in the anterior cingulate gyrus.

The posterior cingulate gyrus plays a part in orientation within and interpretation of the environment, and it has connections and behavioral attributes distinct from those of the anterior cingulate gyrus. Therefore, it is likely that the functions of these divisions are coordinated. The posterior cingulate gyrus also has dense connections with the medial temporal memory system. These communications are

likely to contribute to the role of the posterior cingulate gyrus in orientation. The posterior cingulate gyrus is a major locus that is functionally involved early in the course of Alzheimer's disease. In this study, glucose hypometabolism in DAI patients existed in the whole of the cingulate gyrus as if the phenomena of both aging and Alzheimer's disease occurred at the same time.

The thalamus is also a principal component of the limbic system and the ascending reticular activating system. Therefore, the thalamus has distinct connections with the cingulate gyrus, reticular formation, and cerebral cortex.

There are abundant anatomical connections between the medial parietal region (precuneus)/posterior cingulate and the medial prefrontal region (medial frontal region)/anterior cingulate. These regions are functionally integrated in reflective self-awareness and the resting conscious state.

Axonal damage in the white matter, corpus callosum, and region of the superior cerebellar peduncle is common in patients with DAI. Fibers of the corpus callosum send axon collaterals to the cingulate gyrus. In the present study, glucose hypometabolism was demonstrated bilaterally in the medial prefrontal regions, medial frontobasal regions, cingulate gyrus, and thalamus in every patient with DAI. These results may provide strong evidence that white matter tract disruption, which leads to cortical disconnection resulting in cognitive decline and consciousness disturbance, occurs in patients with DAI.

Acknowledgments The authors thank Seisuke Fukuyama, Yukinori Kasuya, and Ryuji Okumura (Kizawa Memorial Hospital) and Naoki Hirata (General Electric Yokogawa Medical Systems, Tokyo, Japan) for their technical assistance.

References

1. Nakayama N, Okumura A, Shinoda J, et al (2006) Evidence for white matter disruption in traumatic brain injury without macroscopic lesions. J Neurol Neurosurg Psychiatry 77: 850–855.
2. Okumura A, Yasokawa Y, Nakayama N, et al (2005) The clinical utility of MR diffusion tensor imaging and spatially normalized PET to evaluate traumatic brain injury patients with memory and cognitive impairments. No To Shinkei 57:115–122.
3. Miwa K, Shinoda J, Yano H, et al (2004) Discrepancy between lesion distributions on methionine PET and MR images in patients with glioblastoma multiforme: insight from a PET and MR fusion image study. J Neurol Neurosurg Psychiatry 75:1457–1462.
4. Soeda A, Nakashima T, Okumura A, et al (2005) Cognitive impairment after traumatic brain injury: a functional magnetic resonance imaging study using the Stroop task. Neuroradiology 47:501–506.
5. Nakayama N, Okumura A, Shinoda J, et al (2006) Relationship between regional cerebral metabolism and consciousness disturbance in traumatic diffuse brain injury without large focal lesions: an FDG-PET study with statistical parametric mapping analysis. J Neurol Neurosurg Psychiatry 77:856–862.
6. Yasokawa Y, Shinoda J, Okumura A, et al (2007) Correlation between diffusion-tensor magnetic resonance imaging and motor evoked potential in chronic severe diffuse axonal injury. J Neurotrauma 24:163–173.